Applied Physics A (2018) 124:475
https://doi.org/10.1007/s00339-018-1890-0

Applied Physics A
Materials Science & Processing

Effect of incorporation of conductive fillers on mechanical properties and thermal conductivity of epoxy resin composite

Seenaa I. Hussein[1] · Alaa M. Abd-Elnaiem[2] · Tesleem B. Asafa[3] · Harith I. Jaafar[1]

Received: 14 January 2018 / Accepted: 1 June 2018

Abstract
Applications of polymer-based nanocomposites continue to rise because of their special properties such as lightweight, low cost, and durability. Among the most important applications is the thermal management of high density electronics which requires effective dissipation of internally generated heat. This paper presents our experimental results on the influence of graphene, multi-walled carbon nanotubes (MWCNTs) and chopped carbon fibers on wear resistance, hardness, impact strength and thermal conductivity of epoxy resin composites. We observed that, within the range of the experimental data (epoxy resin + 1, 3, 5 wt% of graphene or 1, 3, 5 wt% MWCNT or 10, 30, 50 wt% carbon fibers), graphene-enhanced wear resistance of the nanocomposites by 75% compared to 50% and 38% obtained for MWCNT and carbon fiber composite, respectively. The impact resistance of graphene nanocomposite rose by 26% (from 7.3 to 9.2 J/m^2) while that of MWCNT nanocomposite was improved by 14% (from 7.3 to 8.2 J/m^2). The thermal conductivity increased 3.6-fold for the graphene nanocomposite compared to threefold for MWCNT nanocomposite and a meager 0.63-fold for carbon fiber composite. These enhancements in mechanical and thermal properties are generally linear within the experimental limits. The huge increase in thermal conductivity, especially for the graphene and MWCNT nanocomposites makes the composites readily applicable as high conductive materials for use as heat spreaders and thermal pads.

1 Introduction

Nanocomposite consists of two or more components, one of them being matrix or continuous phase in which nanosized particles are dispersed. These nanoparticles, or nanofillers, constitute the second phase [1]. Generally, nanofillers have a wide range of applications owing to their excellent mechanical and thermal properties which are largely due to the large surface area to volume ratio [2]. Carbonaceous nanofillers such as nanotubes and graphene are thermally conductive and are therefore excellent materials for thermal management of electronics among other applications. Owing to their extremely high power densities, modern microelectronic chips require very high conductive materials for use as gap fillers, heat spreaders, thermal pads and pastes and thermal interface materials. These are vital components of the entire thermal management package and are critical to ensuring good thermal contact between the chips and the metal heat sinks [3].

Graphene has attracted lots of attention due to its unique two-dimensional (2D) structure and novel properties such as zero-gap band structure, high electron mobility [4], high specific area (2600 m^2/g), very high electric conductivity (6000 S/cm) [5], exceptionally high intrinsic thermal conductivity in the range 2000–5000 W/mK near room temperature [6–8], high surface to volume ratio, high aspect ratio, and high strength and modulus [9]. A large volume of the literature is available in this area especially for thermal management of high-density electronics. Renteria et al. reviewed the state-of-the-art in the graphene thermal field where they focused on graphene applications in thermal management based on reported experimental and theoretical data for heat conduction in graphene and graphene nanoribbons during the pre-2014 years [10]. Goli et al. reported that

✉ Alaa M. Abd-Elnaiem
abd-elnaiem@aun.edu.eg

Seenaa I. Hussein
Sinna633@gmail.com

[1] Department of Physics, College of Science, University of Baghdad, Baghdad, Iraq

[2] Physics Department, Faculty of Science, Assiut University, Assiut 71516, Egypt

[3] Mechanical Engineering Department, Ladoke Akintola University of Technology, Ogbomoso PMB 4000, Oyo State, Nigeria

Published online: 07 June 2018

addition of graphene dramatically improves thermal management of Li-ion batteries by lowering the temperature rise within the cells [11]. This is possible because the thermal conductivity of the containing phase change material is significantly enhanced. Similarly, Renteria et al. and Ramirez et al. showed that addition of graphene and graphite fillers improves the thermal conductivity of nanostructured ferrimagnetic iron oxide composites by 2.6 without significantly degrading the magnetization [12, 13]. It was concluded that excellent heat conduction properties of graphene and graphite were responsible for this observation. Saadah et al. incorporated graphene into thermal interface materials to minimize power loss in the solar cell due to overheating [14]. They found that the solar cell temperature was significantly reduced while the open-circuit voltage was enhanced [14].

Like graphene, carbon nanotubes (CNTs) are commonly used as nanoscale fillers for ultra-high-strength reinforcements in high-performance polymer matrix composites following their excellent mechanical properties such as ultra-high Young's modulus (~ 1 TPa) and tensile strength (11–63 GPa) [15, 16]. The extremely high thermal conductivity of the nanotubes led to early expectations that the conductivity of the polymer nanocomposites would also be enhanced by orders of magnitude similar to what is observed with electrical conductivity. Gulotty et al. observed that surface functionalization increases coupling between the carbon nanotube and polymer matrix when MWCNs were functionalized with –COOH groups [17]. They reported that functionalized MWCN simultaneously improve the electrical and thermal properties of the resulting composites [17].

Carbon fiber composite is composed of extremely strong carbon fibers bound by polymers, such as epoxy resin or others. Its high strength-to-weight ratio and rigidity make carbon fiber composite an ideal material for applications in a variety of industries, such as aerospace, automotive and civil engineering, sport and other consumer and technical products [18]. The use of fillers for the enhancement of polymer properties is well documented. Initially, fillers were used to reduce the cost of the polymeric products. However, with time, fillers became an integral part of many applications, particularly for enhancement of mechanical properties of the polymer [19].

It is well established that the properties of nanocomposites are largely dependent on the processing methods and conditions. Among the most common methods are the solution processes; melt blending process; and/or in situ polymerization. The solution mixing consists of three basic steps: dispersion of the filler in a suitable solvent (for example, by ultra-sonication), incorporation of the polymer and finally removal of the solvent by distillation or evaporation [20]. During this process, polymer coats graphene sheets, and when the solvent evaporates, the graphene sheets reassemble, sandwiching the polymer to form a nanocomposite. The compatibility between the solvent, polymer and the filler plays a critical role in achieving good dispersion. The process is applicable for dispersing carbon material within solvents [21].

The melt blending process is a common method particularly used for thermoplastic polymers [22]. The technique employs a high temperature and shear force to disperse fillers in the polymer matrix. High temperature softens the polymer matrix allowing easy dispersion of reinforcing phase. While the process is free from toxic solvent, it is less effective in dispersing graphene in the polymer matrix especially at higher filler loadings due to increased viscosity of the composites [23]. In the in situ polymerization process, the graphene is dispersed through monomers and terminated by polymerization. This approach increases the possibility of using a higher percentage of the filler which might lead to strong interaction with the polymer matrix. This method is largely applicable for preparing nanocomposites with polymers which are not soluble in some solvents or sensible to high temperature [22]. The intercalation of monomers into the layered structure of graphite, during in situ polymerization, increases interlayer spacing which enhances dispersion of graphene in the polymer matrix. This process makes the covalent bonding between the functionalized sheets and polymer matrix via various chemical reactions possible [24].

In the current work, we studied the effect of incorporating conductive fillers (graphene, multi-walled carbon nanotube, and chopped carbon fibers) in the bulk epoxy resin with the objective of improving their mechanical properties and thermal conductivity.

2 Experimental details

2.1 Chemical materials

Epoxy resin (OP105) was procured from Don Construction Products (DCP, Amman, Jordan). While graphene nanopowder (particle size of 6–8 nm) was obtained from Sky Spring Nanomaterials, Inc. (USA), multi-wall carbon nanotubes (MWCNTs, with > 95% purity, outside diameter of 5–15 nm) were purchased from US Research Nanomaterials, Inc.

2.2 Samples preparation

Epoxy hardener solution was formed from three-part epoxy and one-part hardener for optimum crosslinking. The hardener was slowly added to the epoxy resin at room temperature while the mixture was stirred manually for 5 min to minimize agglomeration of filler particles. The composition was left for 24 h at room temperature to dry. Epoxy/graphene, epoxy/carbon nanotube, and epoxy/carbon fiber

composites were prepared by in situ polymerization. For the epoxy/graphene composites; 1, 3, and 5 wt% of graphene were added to the epoxy resin. Ditto for epoxy/carbon nanotube composites. However, 10, 30 and 50 wt% carbon fibers were added to the epoxy resin to form epoxy/carbon fiber composites.

For each case, the resulting solution was heated in a glass tube on a magnetic stirrer at temperature 60–70 °C for 1 h to soften the polymer matrix and allow easy dispersion of reinforcing phase. The solution was thereafter mixed with hardener and stirred vigorously for 5 min. The mixture was then left at room temperature for 24 h. To prepare samples for characterization, the hand-lay-up technique was used to cast the mixture into glass mold ($10\times10\times0.3$ cm^3). The samples were then cut into pieces using 3-cm-diameter Lees Disc (Fig. 1).

2.3 Samples' characterization

The microstructure and dispersion of the composites were investigated using JEOL JSM-5400LV scanning microscope at an accelerating voltage of 15 kV, and the samples' surfaces were coated with sputter-gold to improve the conductivity.

Samples were prepared, according to ASTM, for the following mechanical tests: wear rate, hardness test, and impact strength. These tests were considered because they are largely concerned with the deformation and fracture of materials under applied loading. The resulting properties constitute important consideration during manufacturing of components of machine, vehicles, devices, and structures [25].

The wear test setup consists of an abrasive wear tester, in which the metal wheel (hardness value of 9269 HB) was driven by a motor rotating at 500 revs/min. The metal disc rotated against the fixed specimen, which was in the form of a plate, in the presence of abrasive particles. After a set time of running, the sample was removed, and wear loss was measured. To ensure uniform procedure, contact load, sliding speed (10 mm/s), abrasive particles and its flow rate were kept constant for all the samples. The wear rates (W) were estimated using the following equation [26]:

$$W = \frac{\Delta m}{S_{\mathrm{D}}}, \tag{1}$$

where Δm is the difference in the mass of the sample before and after the test, while S_{D} is the sliding distance which is calculated from the following equation:

$$S_{\mathrm{D}} = 2\pi rnt, \tag{2}$$

where r is the distance of the specimen to the center of the disc, n is a number of sessions of the disk and t is the testing time.

The hardness values of the samples, being mixtures of epoxy resin and fillers, were measured on Shore D Hardness Scale within a range of 0–100. As for the impact strength, the Charpy method was used following the procedure available in ASTM–ISO179. The thermal conductivity coefficient was obtained from the following Lee's Disc experiment equations [27, 28]:

$$K\frac{T_B - T_A}{d_s} = e\left[T_A + \frac{2}{r}\left(d_A + \frac{d_S}{4}\right)T_A + \frac{1}{2r}d_S T_B\right], \tag{3}$$

$$H = IV = \pi r^2 e\left(T_A + T_B\right) + 2\pi re\left[d_A T_A + \frac{d_S\left(T_A + T_B\right)}{2} + d_B T_B + d_C T_C\right], \tag{4}$$

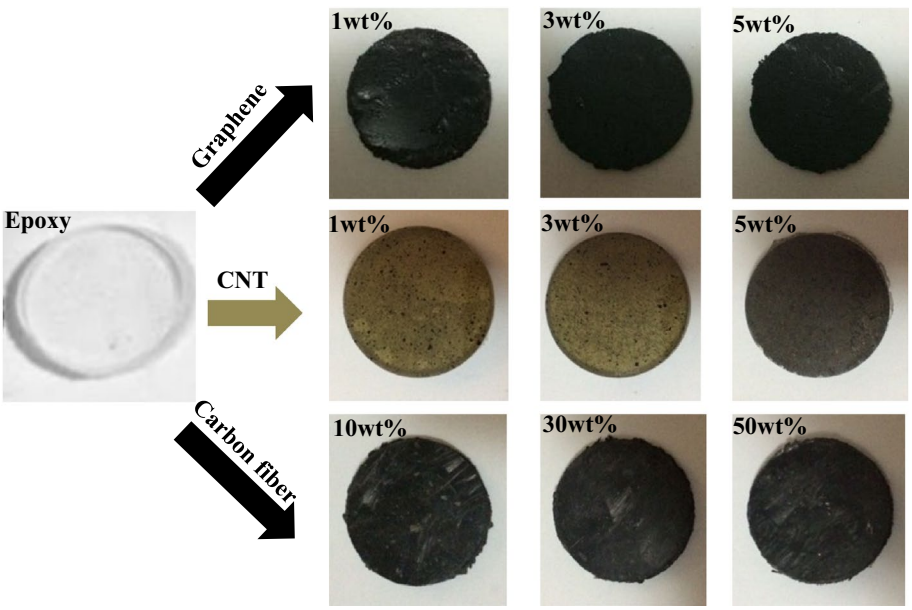

Fig. 1 Samples prepared according to Lee's Disc

where K is the thermal conductivity coefficient, e is the amount of thermal energy passing through a unit area per second of the disc material, H represents the thermal energy passing through the heating coil unit, d is the thickness of the disk (mm), r is the radius of the disk (mm), d_S is the thickness of the sample (mm), T is the temperature of the disk (°C), d_A, d_B, d_C is the thickness of the disk A, B, C, and T_A, and T_B, T_C is the temperature of the disk A, B, C, respectively.

3 Results and discussion

In the current study, different composites were prepared from epoxy with carbon materials as fillers, e.g., graphene, CNT, and carbon fiber, as seen in the optical images in Fig. 1 or SEM images in Fig. 2. The composites were prepared from three different fillers with nine different compositions as can be seen in Fig. 2. The graphene (white particles) amount increases from Fig. 2a to c corresponding to the ratio 1 to 5 wt%. A similar observation can be seen for the CNT filler. For the carbon fiber case, the fiber can be easily seen as observed in Fig. 2h. Generally, the images are indicating a uniform distribution of filer in the epoxy matrix. One can see the filler particles as dispersed particles in the nm–μmscale. The graphene flakes exhibit a nm-scale size increasing by increasing the ratio of graphene. It can be seen that the carbon fiber has smooth surface with a diameter of 6 μm.

The results of the wear rate, impact, strength and thermal conductivity indicate good compatibility of the CNT, graphene and chopped fiber with the epoxy resin. This uniform dispersion is most likely responsible for the uniform results obtained.

3.1 Wear rate

The wear rate as a function of weight ratio under different loads for graphene, carbon nanotube and carbon fibers

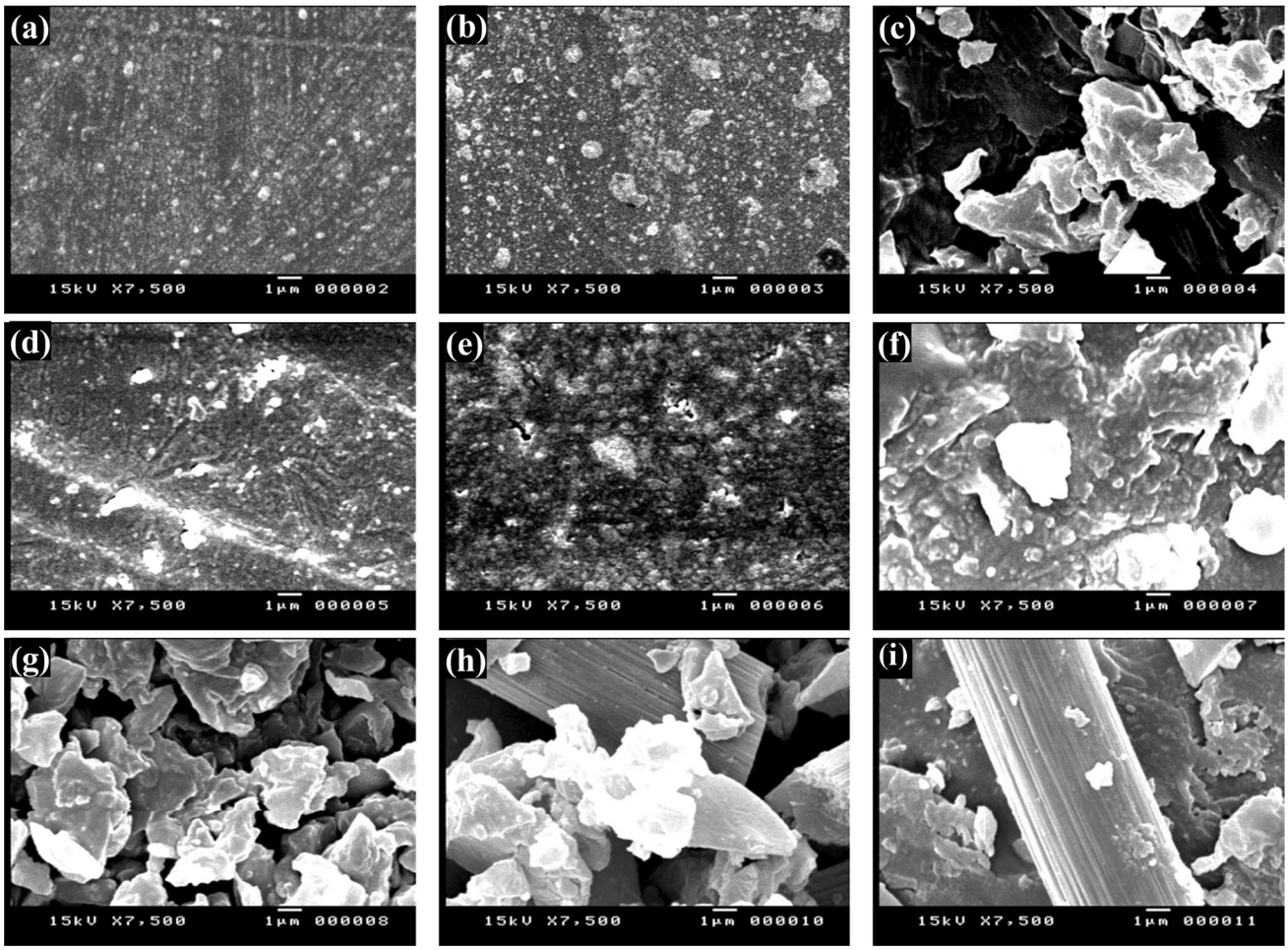

Fig. 2 SEM images show the top view of epoxy-based nanocomposite with **a** 1 wt% graphene, **b** 3 wt% graphene, **c** 5 wt% graphene, **d** 1 wt% CNT, **E** 3 WT% CNT, **f** 5 wt% CNT, **g** 10 wt% carbon fiber, **h** 30 wt% carbon fiber, and **j** 50 wt% carbon fiber

composites are shown in Fig. 3a–c, respectively. The results showed that the wear resistance improved linearly due to the addition of graphene for the three loading conditions considered (Fig. 3a). In other words, the decrease in the friction coefficient of the epoxy composites during sliding is significant.

For 5 N load, the wear rate decreases from 3 g/cm at 0% graphene to 0.8 g/cm for 5% graphene which translates to 73.3%. Similarly, the decrease in the wear rate is about 77 and 76% for 10 and 15 N load, respectively, within the range of graphene used. For similar graphene ratio, wear rate is generally higher for the higher applied force. This behavior could be attributed to the high specific surface of graphene, the solid lubricating effect of graphene sheets [29], strong graphene–epoxy adhesion, interlocking arising from the wrinkled rough surface of graphene and the enhanced glass transition temperature. Compared to other nanofillers such as SiO_2, TiO_2, Al_2O_3 and carbon nanotubes, the effect of graphene was superior in enhancing the wear resistance of epoxy resins at low concentrations. This could be very useful for tribological applications [30]. The observed monotonic increase in wear rate may be due to a monotonic increase in the hardness and Young's modulus of the epoxy composites as reported by Khun et al. [29]. Since hardness and modulus of graphene are higher than those of epoxy, it might be expected that higher fraction of the filler will result in higher hardness. Furthermore, Khun et al. [29] also showed that the friction coefficient of the epoxy composites decreases with increased graphene content. These will consequently lower wear rate.

The wear rate of CNT modified nanocomposite decreases with increased CNT addition reaching a minimum value at about 3% CNT for the three loads considered (Fig. 3b). This then rises for additional CNT indicating that 3% CNT is the optimum addition for best wear reductions estimated as 73, 42 and 36% for 5, 10 and 15 N load, respectively. The initial decrease in the wear rate, up to 3% CNT, is apparently due to the reduction in the friction coefficient of the epoxy composites during sliding while additional CNT makes the composites more brittle and hence higher wear rate [31]. Abdullah et al. observed reduction in wear rate with increased CNT content (from

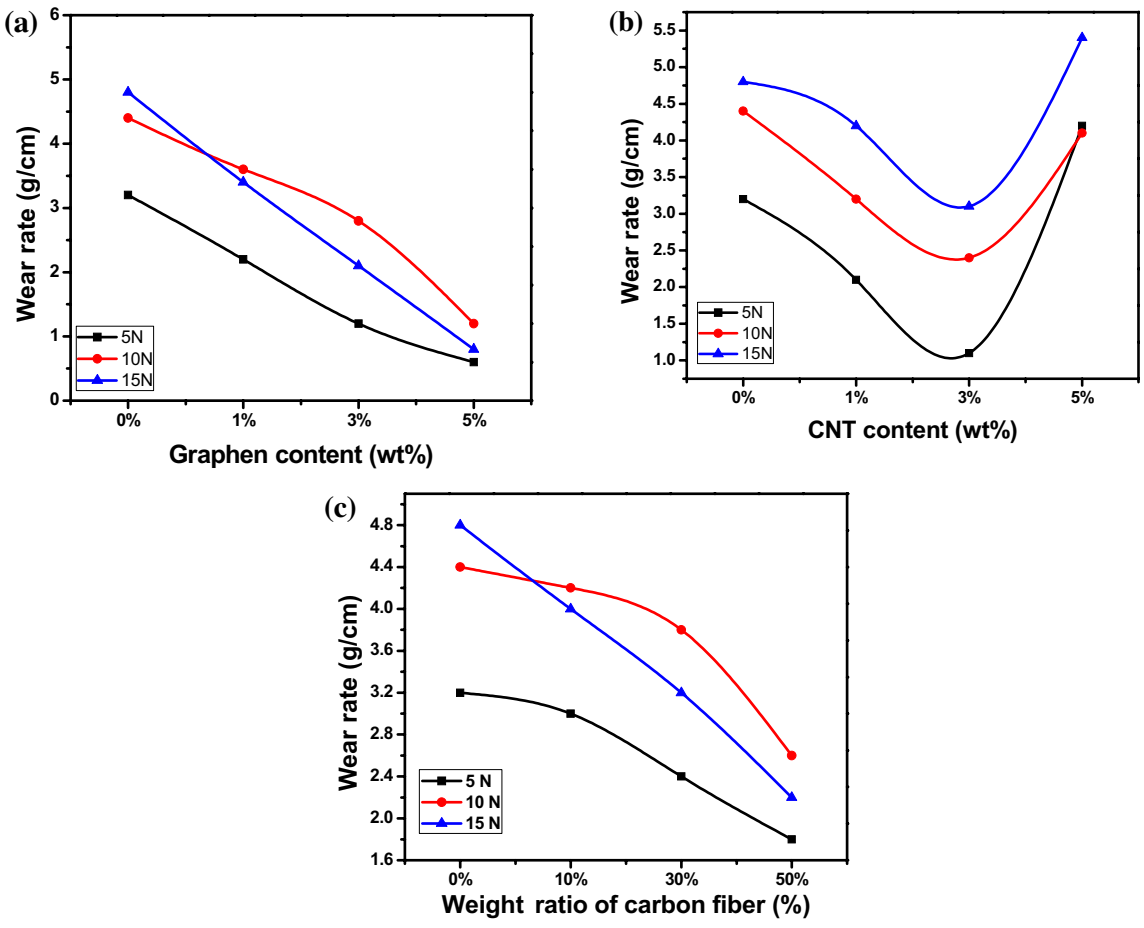

Fig. 3 The wear rate as a function of weight ratio under different loading conditions for **a** graphene, **b** carbon nanotubes (CNT) and **c** carbon fiber (C.F.)

0 to 1.5 wt%) and an increase thereafter (1.5–2 wt%), followed by a rapid increase for the range of CNT content under study. They observed a distinctive abrasive and adhesive type of wear based on the morphological image of the worn surface [32]. It was concluded that the increase in hardness with increased CNT content from 0 to 1.5 wt% followed by a subsequent decrease is responsible for this non-monotonic behavior.

As observed for carbon fiber-modified composite (Fig. 3c), the wear rate decreases, largely linearly, with an increased ratio of chopped carbon fibers. The wear rate decreases from 3 g/cm at 0% carbon fiber to 2 g/cm for 50% fiber for 5 N load, which translates to 33.3% decrease. Moreover, the decrease in the wear rate is about 33% and 48% for 10 and 15 N load, respectively within the range of carbon fiber used. From these results, the addition of graphene enhances wear resistance more than others while carbon fiber offers the least change despite the much higher ratio of added fillers. Generally, the mechanical properties of polymer-based composites are greatly influenced by many factors including the fiber loading, fiber geometry, processing, and the interface between the fiber and matrix [33].

3.2 Hardness and impact strength

The Shore-D hardness values for all the samples are presented in Table 1. This shows that the hardness increases from 72.3 for the pure epoxy resin to 73.6 for epoxy modified with 5 wt% graphene, 73.2 for epoxy with 5% carbon nanotubes and 76.6 for epoxy with 50 wt% chopped carbon fibers. The increased hardness indicates reduced ductility, and consequently, the nanocomposites become more brittle [34].

Impact test reflects the ability of a material to absorb energy before fracture upon exposure to impact load. Figure 4 presents the impact strength of the epoxy nanocomposites indicating that the impact resistance of graphene nanocomposite increased by 26% (from 7.3 to 9.2 J/m^2) while that of CNT nanocomposite is improved by 14% (from 7.3 to 8.2 J/m^2) as the graphene or carbon nanotube content increases from 0 to 3 wt%. This, however, decreases below the impact resistance of pure epoxy as the nanofillers increase beyond 3 wt%. The substantial increase in mechanical performance can be attributed to better covalent bonding between the nanofillers and the epoxy resin. However, at higher graphene content, the fillers get clustered or

Table 1 Shore-D hardness values for epoxy-based composites

Samples	Shore-D hardness value		
	Graphene nanocomposite	Carbon nanotube nanocomposite	Carbon fibers nanocomposite
Pure Ep	72.3	72.3	72.3
EP + 1%Gr or EP + 1%CNT or EP + 10%C.F	72.8	72.5	73.2
EP + 3%Gr or EP + 3%CNT or EP + 30%C.F	76.0	73.8	74.5
EP + 5%Gr or EP + 5%CNT or EP + 50%C.F	73.6	73.2	76.6

EP epoxy resin, *Gr* graphene, *CNT* carbon nanotubes, *C.F.* carbon fibers

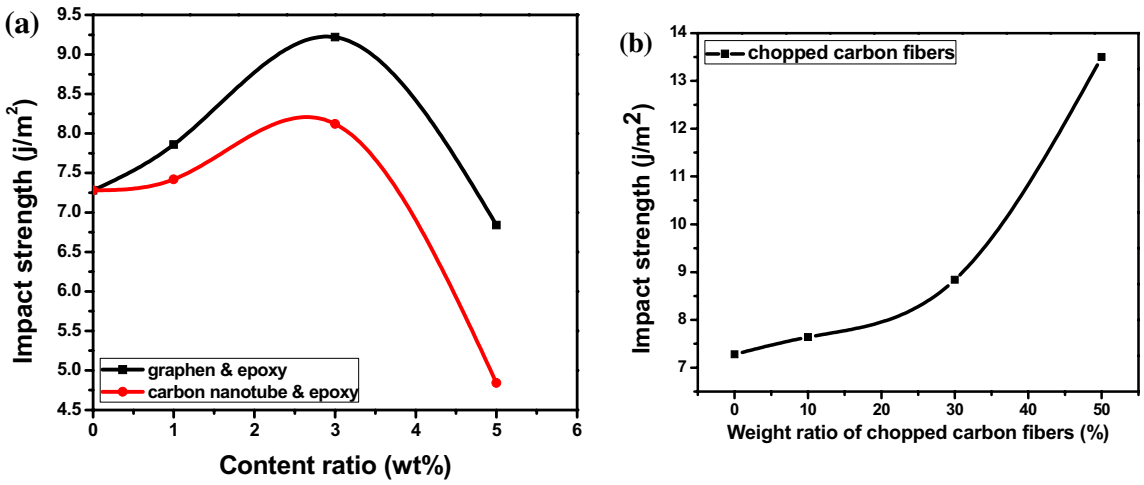

Fig. 4 The impact strength as a function of weight ratio for **a** Graphene and CNT (**b**) Carbon fiber-modified nanocomposites

agglomerated within the epoxy matrix perhaps due to poor dispersion leading to brittle behavior and hence lower impact resistance [35].

Figure 4b shows the impact strength of carbon fibers modified composite. The impact strength increases by 84%, from 7.3 J/m^2 at 0 wt% carbon to 13.4 J/m^2 at 50 wt% fillers. This huge increase is attributed to the weave pattern and longer length of fibers in bi-directional composites which effectively transfer loads from one end to another. Therefore the energy consumed, prior to fracture, due to the regular orientation of fibers and longer fiber is more than that of irregular orientation and short fibers. Furthermore, low strength of short fibers may be attributed to the coexistence of many fibers ends in between the composite and micro-cracks and induced stresses occurs at fiber ends due to impact [36].

3.3 Thermal conductivity

Figure 5 depicts the thermal conductivity of the fabricated nanocomposites. For both graphene and CNT nanocomposites, the thermal conductivity increases linearly with an increased weight fraction of the fillers. At 5 wt% filler loading, the thermal conductivity of the graphene nanocomposite increased by about 3.6-fold (maximum of 0.93 W/mK) while CNT nanocomposite rose by threefold (maximum of 0.8 W/mK) compared to the neat epoxy resin (0.2 W/mK). This observation agrees with the findings reported in Ref [37], as well as 2.6-fold increase observed by Ramirez et al. for nanostructured ferrimagnetic iron oxide composites [13]. A plausible explanation for the observed large increase in the thermal conductivity of graphene/epoxy composites with increased filler content is attributed to the high intrinsic thermal conductivity of graphene (3000–5000 W/mK) as well as good contact between the filler and the matrix. This becomes more significant as the filler loading and dispersion, as well as the thermal resistance of the interface between the fillers and matrix improve [38]. Saadah et al. also reported that graphene fillers are responsible for the improved apparent thermal conductivity of thermal interface materials when used for solar cell application [14]. The slightly lower thermal conductivity

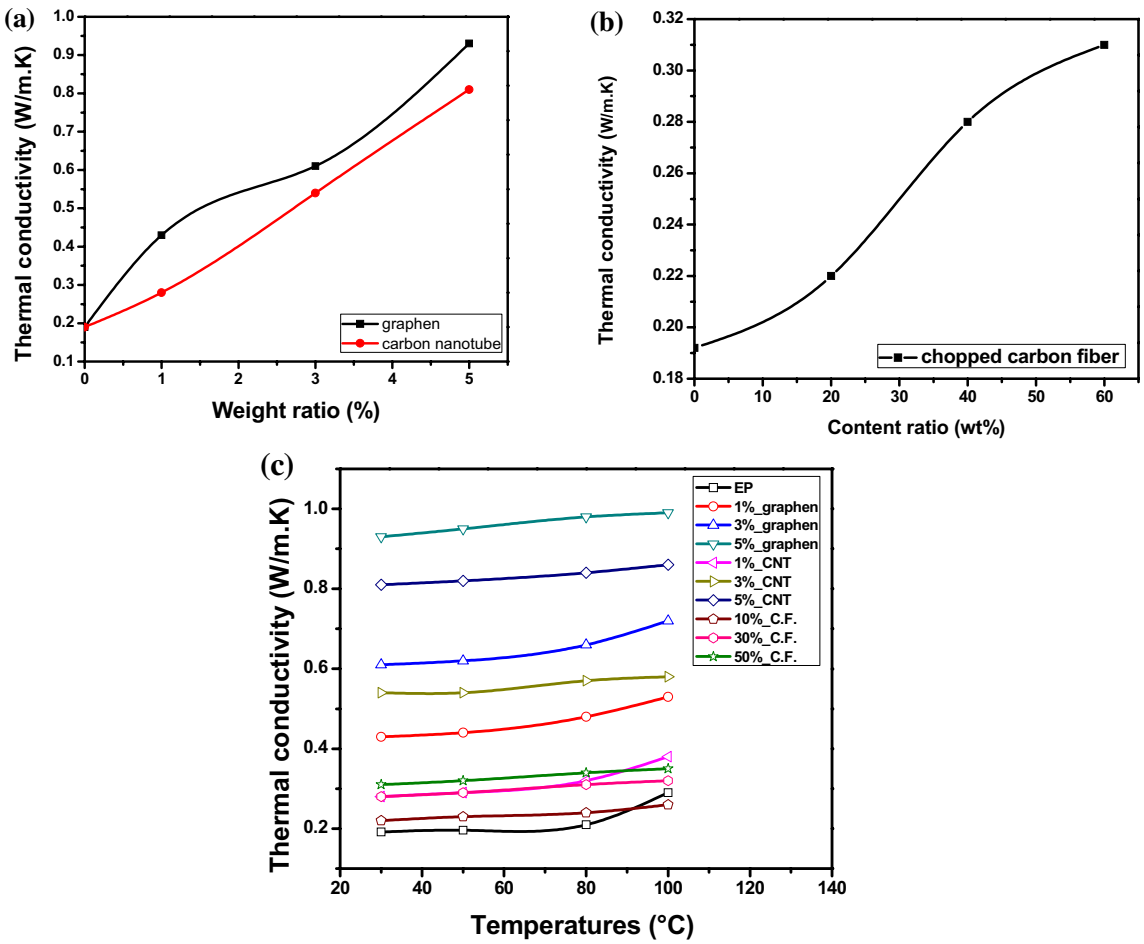

Fig. 5 Thermal conductivity as a function of **a, b** weight ratio, **c** temperature

Table 2 Thermal conductivity of epoxy (EP) composites with graphene, carbon nanotube (CNT), and chopped carbon fibers (C.F.)

Samples	k(W/m K)			
	30 °C	50 °C	80 °C	100 °C
EP	0.192	0.196	0.21	0.23
EP + 1% graphene	0.43	0.44	0.48	0.53
ep + 3% graphene	0.61	0.62	0.66	0.72
ep + 5% graphene	0.93	0.95	0.98	0.99
EP + 1% CNT	0.28	0.29	0.32	0.38
EP + 3% CNT	0.54	0.54	0.57	0.58
EP + 5% CNT	0.81	0.82	0.84	0.86
EP + 10% C.F	0.22	0.23	0.24	0.26
EP + 30% C.F	0.28	0.29	0.31	0.32
EP + 50% C.F	0.31	0.32	0.34	0.35

coefficient of carbon nanotube (3000 W/mK) [39] might be responsible for the slight reduction in the overall thermal conductivity coefficient for the CNT nanocomposites.

For the carbon fiber-modified composite, the thermal conductivity coefficient rose by 63% or just 0.63-fold (Fig. 5b) for 50 wt% carbon fibers. In spite of the high volume of carbon fiber added, the thermal coefficient is still far below those of graphene- or CNT-modified nanocomposites. This result can be explained by the fact that the carbon fiber is randomly orientated with far lower thermal conductivity coefficient (15 W/mK) compared to the other fillers [39].

Since epoxies are poor thermal conductors, fibers must be introduced into the matrix to enhance the thermal transfer within the composite. The contribution of the fillers to the thermal conductivity depends on their nature, loading, and dispersion. The process of thermal energy transfer depends on the structural nature of the material under consideration. Thermal energy can be transferred either by lattice waves or free electrons (photons). In insulating materials, thermal energy is transmitted by phonons as molecules oscillate [40]. The modification of epoxy matrix might have caused a decrease in the mean distance between neighboring chains of the epoxy resin as fillers take interstitial positions. Consequently, thermal resistance decreases. This huge increase in thermal conductivity, especially for the graphene and CNT nanocomposites makes the composite readily applicable as high conductive materials for use as heat spreaders and thermal pads.

Figure 5 and Table 2 show the variation of thermal conductivity as a function of test temperature for all the composites. The results show that the thermal conductivity increases linearly but weakly with increased test temperature. A similar observation was reported by Goli et al. in which the weak dependence is attributed to the disordered nature of the composite which is obtained when graphene is mixed randomly with the matrix [11]. For functionalized MWCNT, Gulotty et al. observed initial rise followed by fall in thermal conductivity at a temperature greater than 40 °C [17]. The observed slight increase in temperature, according to our results, is expected because of intermolecular vibrations (which is a measure of thermal conductivity) increase with temperature [41]. Since interatomic vibrations increase about the mean position, entropy increases as molecules gain more energy allowing heat to be transmitted through the vibrating molecules easier and faster [42]. The thermal conductivity of composites with random fillers increases with temperature, which is characteristic of amorphous and disordered materials [11].

4 Conclusion

The effects of addition of graphene, carbon nanotubes and carbon fibers to epoxy resin on mechanical and thermal properties of the resulting composites were investigated and reported. Increasing the graphene, carbon nanotube and carbon fiber reduces wear rate significantly. These fillers also enhance the hardness and impact strength of the composites. The influence of the filler on thermal conductivity is very significant as it was enhanced 3.6-fold by graphene and threefold by CNT. In addition, the thermal conductivity increases with temperature for all samples within the experimental limit.

References

1. F.A. dos Santos, G.C. Iulianelli, M.I.B. Tavares, Mater. Sci. Appl. **7**, 257 (2016)
2. C. Huang, W. Zhen, Z. Huang, D. Luo, Appl. Phys. A **124**, 38 (2018)
3. N.K. Mahanta, M.R. Loos, I.M. Zlocozower, A.R. Abramson, J. Mater. Res. **30**, 959 (2015)
4. A. Li, C. Zhang, Y.F. Zhang, Polymers **9**, 437 (2017)
5. A.K. Geim, S.N. Konstantin, Nat. Mater. **6**, 183 (2007)
6. A.A. Balandin, S. Ghosh, W. Bao, I. Calizo, D. Teweldebrhan, F. Miao, C.N. Lau, Nano Lett. **8**, 902 (2008)
7. A.A. Balandin, Nat. Mater. **10**, 569 (2011)
8. D.L. Nika, A.A. Balandin, Rep. Prog. Phys. **80**, 036502 (2017)
9. J. Wei, R. Atif, T. Vo, F. Inam, J. Nanomater. **16**, 374 (2015)
10. J.D. Renteria, D.L. Nika, A.A. Balandin, J. Appl. Sci. **4**, 525 (2014)
11. P. Goli, S. Legedza, A. Dhar, R. Salgado, J. Renteria, A.A. Balandin, J. Power Sources **248**, 37 (2014)
12. J. Renteria, S. Legedza, R. Salgado, M.P. Balandin, S. Ramirez, M. Saadah, F. Kargar, A.A. Balandin, Mater. Des. **88**, 214 (2015)
13. S. Ramirez, K. Chan, R. Hernandez, E. Recinos, E. Hernandez, R. Salgado, A.G. Khitun, J.E. Garay, A.A. Balandin, Mater. Des. **118**, 75 (2017)
14. M. Saadah, E. Hernandez, A.A. Balandin, Appl. Sci. **7**, 589 (2017)
15. S. Iijima, Nature **354**, 56 (1991)
16. B. Arash, Q. Wang, V.K. Varadan, Sci. Rep. **4**, 6479 (2014)
17. R. Gulotty, M. Castellino, P. Jagdale, A. Tagliaferro, A.A. Balandin, ACS Nano **7**, 5114 (2013)

18. J. Wu, Z. Kou, G. Cui, Ind. Lubr. Tribol. **68**, 212 (2016)
19. M. Bhattacharya, Materials **9**, 262 (2016)
20. X. Huang, X. Qi, F. Boey, H. Zhang, Chem. Soc. Rev. **41**, 666 (2012)
21. T. Kuilla, S. Bhadra, D. Yao, N.H. Kim, S. Bose, J.H. Lee, Prog. Polym. Sci. **35**, 1350 (2010)
22. H. Ago, K. Petritsch, M.S. Shaffer, A.H. Windle, R.H. Friend, Adv. Mater. **11**, 1281 (1999)
23. V. Singh, D. Joung, L. Zhai, S. Das, S.I. Khondaker, S. Seal, Prog. Mater Sci. **56**, 1178 (2011)
24. D. Galpaya, M. Wang, M. Liu, N. Motta, E.R. Waclawik, C. Yan, Graphene **1**, 30 (2012)
25. I. Engelberg, J. Kohn, Biomaterials **12**, 292 (1991)
26. R. owicy, *"Fraction and wear of materials"* (Wiely, New York, 1965)
27. E.S. Al-Hassani, Eng Tech J, **28**, (2010) (1982)
28. F.A. Saleh, F.A. Abdulla, A.A.J. Mahdi, J. Eng. Dev. **19**, 147 (2015)
29. N.W. Khun, H. Zhang, L.H. Lim, J. Yang, KMUTNB: IJAST **8**, 101 (2015)
30. X. Li, H. Gao, W.A. Scrivens, D. Fei, X. Xu, M.A. Sutton, A.P. Reynolds, M.L. Myrick, Nanotechnology **15**, 1416 (2004)
31. M. Cho, Mater. Trans. **49**, 2801 (2008)
32. U. Abdullahi, M.A. Maleque, U. Nirmal, Procedia Eng. **68**, 736 (2013)
33. Y. Şahin, P. De Baets, I.O.P. Conf, Ser. Mater. Sci. Eng. **174**, 012009 (2017)
34. J.N. Coleman, U. Khan, W.J. Blau, Y.K. Gun'ko, Carbon **44**, 1624 (2006)
35. N. Norhakim, S.H. Ahmad, C.H. Chia, N.M. Huang, Sains Malays. **43**, 603 (2014)
36. G. Agarwal, A. Patnaik, R.K. Sharma, J. Eng. Sci. Technol. **9**, 590 (2014)
37. J. Wei, T. Vo, F. Inam, RSC Adv. **5**, 73510 (2015)
38. Y. Wang, J. Yu, W. Dai, Y. Song, D. Wang, L. Zeng, N. Jiang, Polym. Compos. **36**, 556 (2015)
39. F.T. Fisher, R.D. Bradshaw, L.C. Brinson, Appl. Phys. Lett. **80**, 4647 (2002)
40. T.L. Bergman, F.P. Incropera, D.P. DeWitt, A.S. Lavine, *Fundamentals of heat and mass transfer*, (Wiely, New York, 2011)
41. E. Piokowska, A. Goleski, Int. Polym. Sci. Tech. **12**, 102 (1985)
42. J. Hone, M.C. Llaguno, M.J. Biercuk, A.T. Johnson, B. Batlogg, Z. Benes, J.E. Fischer, Appl. Phys. A **74**, 339 (2002)